Available online at www.sciencedirect.com
ScienceDirect
Journal of Nuclear Materials 360 (2007) 272–281
journal of nuclear materials
www.elsevier.com/locate/jnucmat

Study of radiation-induced degradation of RPV steels and model alloys by positron annihilation and Mössbauer spectroscopy

Andrej Zeman [a,*], Luigi Debarberis [a], L'udovít Kupča [b], Beatriz Acosta [a], Miloš Kytka [c], Jarmila Degmová [a,d]

[a] European Commission, Joint Research Centre, Institute for Energy, P.O. Box 2, 1755ZG Petten, The Netherlands
[b] VÚJE plc., Okružná 5, 918 64 Trnava, Slovakia
[c] Nuclear Research Institute Řež plc., Husinec – Řež 130, 250 68 Řež, Czech Republic
[d] Department of Nuclear Physics and Technology, Slovak University of Technology, Ilkovičova 3, 81219 Bratislava, Slovakia

Received 12 June 2006; accepted 24 October 2006

Abstract

The influence of different microstructural processes on the degradation due to radiation embrittlement has studied by positron annihilation and Mössbauer spectroscopy. The materials studied consisted of WWER-440 base (15Kh2MFA) and weld (10KhMFT) RPV steels which were neutron-irradiated at fluence levels of $0.78 \times 10^{24}\ m^{-2}$, $1.47 \times 10^{24}\ m^{-2}$ and $2.54 \times 10^{24}\ m^{-2}$; WWER-1000 base (15Kh2NMFAA) and weld (12Kh2N2MAA) irradiated at a fluence level $1.12 \times 10^{24}\ m^{-2}$; three different model alloys implanted with protons at two dose levels (up to 0.026 dpa), finally the base metal of WWER-1000 (15Kh2NMFAA) was thermally treated with the intention to simulate the P-segregation process. It has been shown possible to correlate the values of parameters obtained by such techniques and data of mechanical testing (ductile-to-brittle transition temperature and upper shelf energy).

1. Introduction

A main objective for the EU nuclear-industry is to maximize and enhance the safety and the reliability of nuclear power plants (NPP) and to extend their operation lifetime. The reactor pressure vessel (RPV) is one of the most critical elements with the highest priority in safety rankings. Therefore it is closely monitored and tested by surveillance programmes. The RPV is not practically and economically replaceable and as it is subject to significant usage degradation it often becomes the component determining the operational safety of the NPPs. The ageing and irradiation related degradation mechanisms of RPV steels are very complex processes dependent on many factors. Additionally their interaction with irradiation hardening and embrittlement is not yet fully understood. Hence, beside of mechanical testing used for structural integrity analysis of RPV steels, non-destructive

* Corresponding author. Tel.: +31 224 565467; fax: +31 224 565636.
E-mail address: Andrej.Zeman@jrc.nl (A. Zeman).

0022-3115/$ - see front matter © 2006 Elsevier B.V. All rights reserved.
doi:10.1016/j.jnucmat.2006.10.011

techniques (NDT) are applied to provide further sight into the microstructured evolution.

The degradation of RPV steel is a very complicated process dependent on many factors (thermal treatments and radiation exposure, chemical composition, fabrication and post-production processing conditions, etc.). This topic has been the subject of many comprehensive studies [1–6]. However, the related neutron embrittlement and microstructural changes remain only partially understood. The effect of intense fluxes of neutrons results in considerable changes of a materials structure and properties. In particular, the development of fine scale radiation-induced defects, which impede dislocation motion under applied stress, leads to degradation of mechanical properties, which can result in hardening and possibility of brittle fracture. This process is known as irradiation embrittlement [7]. Defects are formed from vacancies and interstitials created in cascaded collision processes. Those point defects surviving the cascades migrate freely through the crystal lattice, interacting with each other, with solute atoms in the matrix and also with the dislocation substructure and precipitates. These irradiation-induced diffusion processes result in the formation of new point defect clusters, dislocation loops and precipitates [8].

The neutron embrittlement of RPV steels is a pronounced problem in Russian WWER types of nuclear reactors. It is generally accepted that even in the Western RPV steel types containing more than 0.1 wt% of Cu, Cu- and P-rich precipitates play a dominant role in thermal and neutron embrittlement. In the case of WWER-type RPV steels, several studies [9–14] have suggested that carbide formation is an important additional microstructural mechanism. The contribution of Ni content to irradiation hardening and embrittlement was until recently not fully realised. The Ni effect has been observed in RPV steel plates and forgings, as well as welds. It was shown that this effect is important for steels with Ni contents higher than 0.4 wt%. Materials with high Cu and Ni contents have a high irradiation sensitivity while those with low Cu and Ni content are practically insensitive to irradiation [9]. Most of the published data show that the Ni effect is very dependent on the Cu content, and the Ni content does not appear to play any role when the Cu content is low (<0.1 wt%). This suggests the existence of a synergetic mechanism resulting from interactions between Cu and Ni [9–11].

Generally, the processes that play a dominant role in the mechanism of radiation embrittlement, are (i) direct matrix damage (DMD), (ii) precipitation hardening and (iii) segregation process (Fig. 1). The different semi-mechanistic models for prediction of WWER RPV steels have been taken into the consideration. The recently published a semi-mechanistic model (1) of radiation damage [12] and standard models for WWER-440 (2) and WWER-1000 (3) according to the Russian Guides

$$\Delta T_{\mathrm{K}} = a \cdot \Phi^{n} + b \cdot (1 - \mathrm{e}^{-\Phi/\Phi_{\mathrm{sat}}}) + c \cdot \left[0.5 + 0.5 \cdot \tanh\left(\frac{\Phi - \Phi_{\mathrm{sat}}}{d}\right)\right], \quad (1)$$

$$\Delta T_{\mathrm{K}} = 800 \cdot (\mathrm{P} + 0.07 \cdot \mathrm{Cu}) \cdot \Phi^{1/3}, \quad (2)$$

$$\Delta T_{\mathrm{K}} = [230 \cdot (\mathrm{Cu} + 10\mathrm{P}) + 20] \cdot \Phi^{1/3}, \quad (3)$$

where a, b, c, P and Cu are the parameters, n is the exponent and Φ is the neutron fluence.

The application of additional methods to assess the embrittlement is essential for better understanding of these damage mechanisms at microstructural level. Very few techniques are capable to detect of defects at the atomic level; moreover it is extremely difficult to study the interaction of defects and the contribution of alloying elements to the kinetics of radiation damage at the experimental base. Nuclear methods, such as positron annihilation or Mössbauer spectroscopy, in combination with transmission electron microscopy (TEM) can be very helpful in this, as confirmed by recently published data [10,13,14]. Some characteristics of positron lifetime parameters for defects in iron and carbides are specified in Table 1. An example of lifetime spectra is shown in Fig. 2(a). The level of uncertainty for

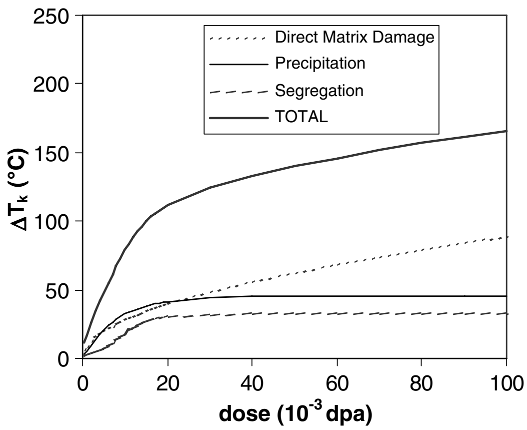

Fig. 1. Semi-mechanistic analytical model of the radiation embrittlement for WWER-1000 base metal.

Table 1
Positron lifetime parameters for different types defect in pure iron and in carbides of Cr–Mo–V steels

Material	Lifetime (ps)	References
Fe-bulk	110	[15]
Fe-dislocations	165	[16]
Fe-monovacancy	175	[15]
Fe-divacancy	197	[16]
Fe-3 vacancy cluster	232	[16]
Fe-4 vacancy cluster	262	[16]
Fe-6 vacancy cluster	304	[16]
VC	99	[17]
$V_{0.86}Cr_{0.09}Mo_{0.04}Fe_{0.01}C$	105	[17]
Mo_2C	112	[17]
$Mo_{1.4}Cr_{0.6}C$	116	[17]
Cr_7C_3	107	[17]
$Cr_{23}C_6$	112	[17]
$Mn_{26}C_6$	99	[17]
Fe_3C	101	[17]

identification of particular defects by positron lifetime is higher for complex systems, such as RPV steels, which contain many alloying elements and impurities. Therefore, parallel studies in more simple systems (binary, ternary, quaternary model alloys) are essential.

2. Experiments

The testing of the RPV WWER-1000 base and weld metals has been performed by European Commission, Joint Research Centre, Institute for Energy Petten (Netherlands) and Nuclear Research Institute Rez (Czech Republic) in frame of the IAEA Coordinated Research Programmes (CRP) [9]. The data for RPV WWER-440 base and weld metal have been collected from recently published studies [18–21] of surveillance programmes.

2.1. Techniques

For the investigation of WWER steels and RPV model alloys positron annihilation spectroscopy (PAS) and Mössbauer spectroscopy (MS) were chosen. This part of research was carried out as a joint study by European Commission, Joint Research Centre, Institute for Energy Petten and Slovak University of Technology Bratislava. The measurements were performed using both conventional lifetime fast-slow system and a pulsed low energy positron system (PLEPS) [10,22]. The time resolution of this experimental device is 240 ps FWHM (full width at half maximum). The principle of positron lifetime measurement is based on the registration period between the birth of the positron in the ^{22}Na source (1274 keV start phonon or electronically controlled pulse PLEPS) and its annihilation in the bulk of the studied material (511 keV stop phonon). This technique was upgraded for the measurement of irradiated specimens and enables the study of the microstructural changes in the region from 20 to 510 nm (depth profiling) with a specimen thickness of 50 μm, thus minimising the ^{60}Co radiation contribution which disturbs the lifetime spectra. At least 3×10^7 counts per spectrum were collected. Data post-processing and spectra analysis were performed by the software program LT9. For the analysis, it can be considered that the positron annihilation lifetime spectroscopy (PALS) is a well-established method for studying open-volume type atomic defects and

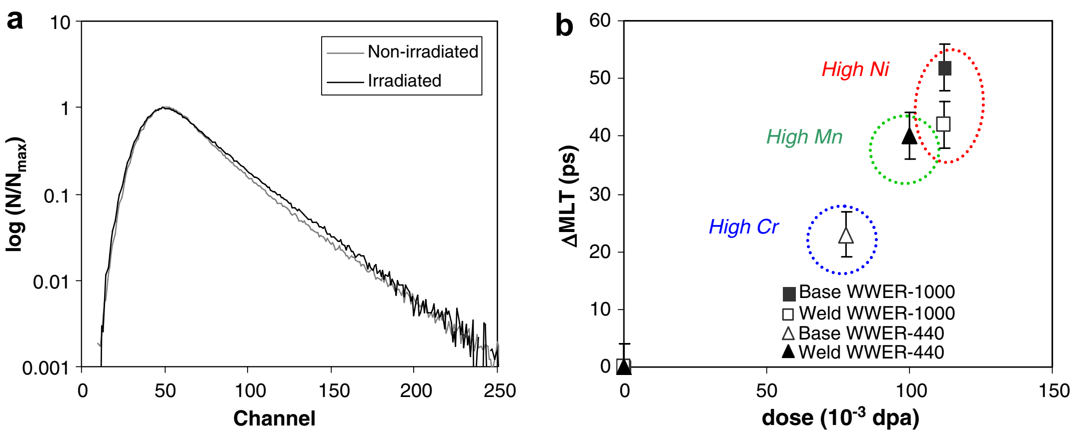

Fig. 2. (a) Normalised positron lifetime spectra of WWER-440 weld metal in unirradiated and irradiated conditions (fluence: 1.47×10^{24} m^{-2}), (b) MLT parameter versus dose for WWER-440/WWER-1000 base and weld metals.

defect impurity interactions in metals and alloys. The lifetime of positrons trapped at vacancies, vacancy-impurity pairs, dislocations, microvoids, etc. is longer than that one of free positrons in the perfect region of the same material. As a result of the presence of open-volume defects, the average positron lifetime observed in structural materials is found to increase with damage [1,3,4].

The measurements by Mössbauer spectroscopy is based on the Mössbauer effect of resonance absorption of gamma radiation. The spectrometer with transmission geometry, a standard constant acceleration and a ^{57}Co source in a rhodium matrix were used. All measurements were performed at room temperature with statistics about 1.5×10^6 counts per channel. The test specimens consisted of 20–30 μm thick foils of the materials being investigated. The 4-sextets model was applied for the spectra analysis.

3. Results

3.1. Effect of neutron irradiation

The WWER-440 RPV base and weld metals have been irradiated as a part of the surveillance programme of NPP Bohunice (Slovakia) at fluence levels of $0.78 \times 10^{24}\ \mathrm{m^{-2}}$, $1.47 \times 10^{24}\ \mathrm{m^{-2}}$ and $2.54 \times 10^{24}\ \mathrm{m^{-2}}$ ($E_n > 0.5$ MeV, $T_{irr} = 275$ °C). The samples of WWER-1000 steel were irradiated in the experimental reactor LVR-15 at NRI Rez (Czech Republic) at a fluence of $1.12 \times 10^{24}\ \mathrm{m^{-2}}$ ($E_n > 0.5$ MeV, $T_{irr} = 290$ °C). The chemical composition of the WWER RPV steels is specified in Table 2.

The mean lifetime parameter (MLT) increases with the density of vacancy-type defects (mono-vacancies, di-vacancies, open volume defects, Frenkel pairs and dislocation lines). According to the mean lifetime analysis of the results and the comparison of all four RPV steels in the un-irradiated state, it can be concluded that the concentration of defects in the specimens is relatively high. The MLT value of about 165–175 ps indicates that the samples have been affected during the fabrication process from the microstructural point of view and dislocations as well as point defects and their clusters probably have been generated in the material structure. However, after annealing of the unirradiated samples (475 °C, 10^{-6} Pa vacuum) the MLT value decreased to the level 120–140 ps (in comparison the MLT of pure iron is about 110 ps). Nevertheless, according to the MLT analysis, irradiation mainly causes the creation of point

Table 2
Chemical composition of alloying elements and impurities (wt%) and mechanical parameters (DBTT, USE) of unirradiated WWER-440 and WWER-1000 RPV steels

Element/ Parameter	WWER-1000 BM (15Kh2NMFAA)	WWER-1000 WM (12Kh2N2MAA)	WWER-440 BM (15Kh2MFA)	WWER-440 WM (10KhMFT)
C	0.16	0.11	0.14	0.048
Si	0.29	0.14	0.31	0.37
Mn	0.42	0.73	0.37	1.11
Cr	1.97	1.9	2.64	1.00
Ni	1.29	1.7	0.20	0.12
Cu	0.12	0.08	0.091	0.103
S	0.008	0.008	0.017	0.013
P	0.012	0.006	0.014	0.043
V	0.10	0.01	0.27	0.13
Mo	0.52	0.55	0.58	0.39
Al	0.003	–	–	–
Sb	0.001	–	0.005	–
Co	0.006	0.009	0.019	0.020
As	0.003	0.008	0.001	–
Sn	0.003		0.005	–
$T_{41\,J}$ (°C)	−70.1	−57.8	−54.4	10.1
USE (J)	195.6	95.6	204.6	136
$F_{LT}\ (\mathrm{m^{-2}})_{E_n > 1\,\mathrm{MeV}}$	3.7×10^{23}	3.7×10^{23}	2.4×10^{24}	1.6×10^{24}

DBTT – ductile to brittle transition temperature.
USE – upper shelf energy.
F_{LT} – lifetime fluence for RPV.

defects as well enabling their mobility in the material due to irradiation temperature at the levels 275 °C and 290 °C, respectively. The ΔMLT is in the range 20–50 ps. It seems that WWER-1000 RPV steels with higher concentration of nickel (15Kh2NMFAA and 12Kh2N2MAA) are more sensitive to the generation of microstructural defects (vacancy type). On the other hand, the behavior of WWER-440 RPV steels (15Kh2MFA and 10KhMFT) is rather different. This effect of different behavior is related probably to the interaction with the manganese and chromium. Based on the analysis of lifetime parameters, we can assume the 15Kh2MFA RPV steel has a better resistance to the radiation damage (Fig. 2(b)) than the other WWER steels studied from microstructural point of view.

Moreover, recently published results from atom probe field ion microscopy (APFIM) confirms the presence of solute-rich precipitates in irradiated RPV steels, which are formed in small clusters with non-random distributions within the matrix [9]. We can assume that solute-related damage also contributes to the direct matrix damage. However, it is not possible yet to distinguish this contribution from lifetime parameters yet. An significant correlation between the MLT parameters and ductile-to-brittle transition temperature ($T_{41\,\mathrm{J}}$) and upper shelf energy (USE) parameter was observed (Fig. 3). More experimental studies are needed to clarify the role of manganese and chromium in the kinetics of radiation damage and contribution of solute-rich preciptates. Recently published data for WWER-440 materials [23] shows that chromium can drastically reduces the radiation sensitivity. Research on this issue is ongoing within the frame of PRIMAVERA international project.

Mössbauer spectra of unirradiated and irradiated RPV steels (10KhMFT and 12Kh2N2MAA) are shown in Fig. 4. All the samples showed typical Mössbauer spectra for this type of steel with low alloy-element concentrations. The main features are the presence of four magnetically split sub-spectra with isomer and quadrupole shifts close to 0 mm/s and, in certain cases a weak superimposed doublet component (as its contribution is on the level of only 1%; we have neglected it). For the first sextet, the hyperfine field H_{hf1} was fixed at the level of 33.0 T (Fe-atoms in pure iron matrix not surrounded by foreign atoms in their close-neighbour shells). The changes of the relative area parameters (A_{rel1} and A_{rel2}) with $T_{41\,\mathrm{J}}$ and USE are summarised in Fig. 5.

The second and third sextets with hyperfine fields H_{hf} of about 33.6 T and 30.6 T, respectively, can be attributed to the influence of alloying elements which are in the first neighbourhood of Fe-atoms. The fourth sextet (H_{hf} of about 30.1 T and 28.5 T) is associated with iron atoms surrounded in their second or next-neighbour shells by alloying elements. The hyperfine fields remained almost stable for all irradiated or annealed specimens. Therefore, we focused our attention to the changes in the A_{rel} parameter (relative area describing the contribution of this sub-spectrum to the whole spectrum, see Fig. 5).

3.2. Non-hardening embrittlement of phosphorus-segregated RPV steel

In addition to the irradiation embrittlement, a special heat treatment was performed on selected

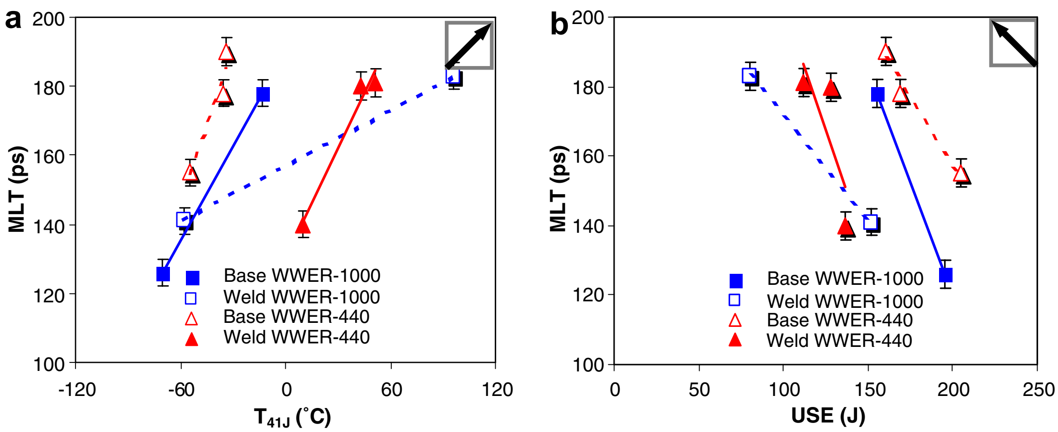

Fig. 3. (a) Change of the MLT parameter with $T_{41\,\mathrm{J}}$, (b) MLT correlation with USE for WWER RPV steels after irradiation. Arrow indicates the trend-line after irradiation.

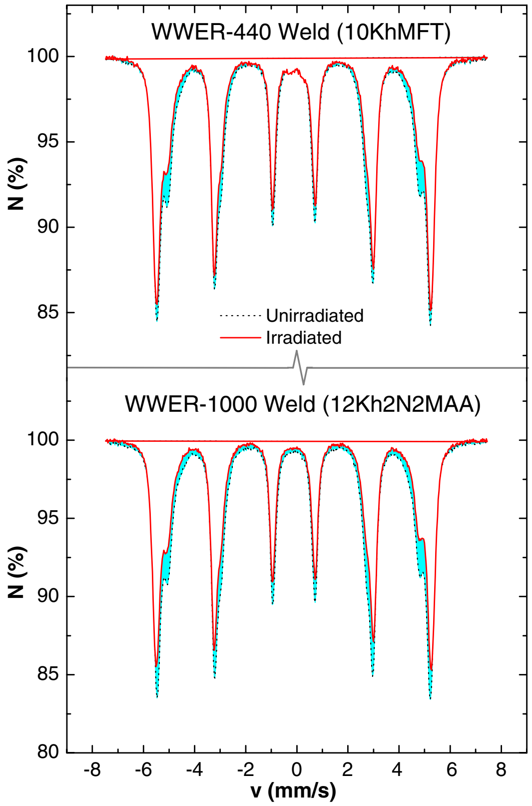

Fig. 4. Mössbauer spectra of WWER-440 and WWER-1000 weld metals in unirradiated and irradiated conditions (fluence: 1.47×0^{24} m^{-2} and 1.12×10^{24} m^{-2}, respectively).

WWER-1000 RPV base metal (15Kh2NMFAA) with the aim of inducing the phosphorus segregation (Table 3), as well as other known segregating impurities (As, Sb, Sn, S, etc.), relying on specific Russian knowledge and availability of dedicated time-temperature plots (Fig. 6(a)). However, no significant change in the hardness of 15Kh2NMFAA steel was registered due to the segregation process. Only the Charpy-V (CV) impact testing indicated significant degradation demonstrating that non-hardening embrittlement (Fig. 6(b)) occurs due to segregation ($\Delta T_{41\,J}$ up to 83 °C). Moreover, only a very slight increase of the MLT parameter (4–5 ps) was registered. Therefore, we have to assume that sensitivity of PAS to the P-segregation simulated by thermal treatment is limited.

3.3. Determination of chemical composition effects on embrittlement

Three different model alloys were selected for the investigation in order to study the contribution of different alloying and impurity elements and their role in irradiation hardening and embrittlement. The specifications of the selected model alloys, together with their mechanical properties, are given in Table 4. The proton treatment was applied to simulate radiation damage and embrittlement, which is induced by neutrons in real RPV materials. A displacement-per-atom (dpa) parameter was used in order to characterise the radiation damage (Table 5). The dpa parameter was adjusted only for the sample volume (Dose_{LT}), which is reachable by positrons emitted from ^{22}Na source. These values seem to be more representative, as the original ones were calculated for the whole sample volume.

The two-components and MLT analyse was performed for the lifetime spectra evaluation. A lifetime τ_1 value of about 110 ps is the dominant low-alloyed steel component with an intensity I_1 of about 80%. This component is assigned to the bulk properties and is slightly influenced by small defects. The second component τ_2 with intensity $I_2 < 20$–25% and value of about 220–350 ps can be attribute to the contribution of large vacancy type defects and/or small clusters of vacancies. It was found that the positron mean lifetime increases with Ni and Cu contents. The proton bombardment caused an increase in the MLT parameter with the dpa level due to primary-knockout-atom (PKA) movements (Fig. 7(a)). The most significant increase of the MLT parameter at the first implantation level (about 0.01 dpa) was detected for MA-635. According to the intensities of the two dominant lifetime components, it seems that larger defect agglomerations are systematically created after proton bombardment, while their density decreases. An increase of MLT values up to about 150 ps after implantation hints at higher annihilation rate in defects concentrated at dislocation lines. This can be deduced from comparison of the results from the MLT and 2-components analyse. The intensity I_2 is significantly reduced with the implantation level. In contrast, the MLT and τ_2 values significantly increase due to proton irradiation. Therefore, we can assume that incubated vacancy types of defect join to bigger conglomerates, such as vacancy clusters. Afterwards, those formations probably migrate and can be attached at the area of dislocation loops.

From the comparison of the already published data for neutron irradiated model alloys [11] and PAS results it was established that damage mechanism in the model alloy MA-175 (Fig. 7(b)) can be

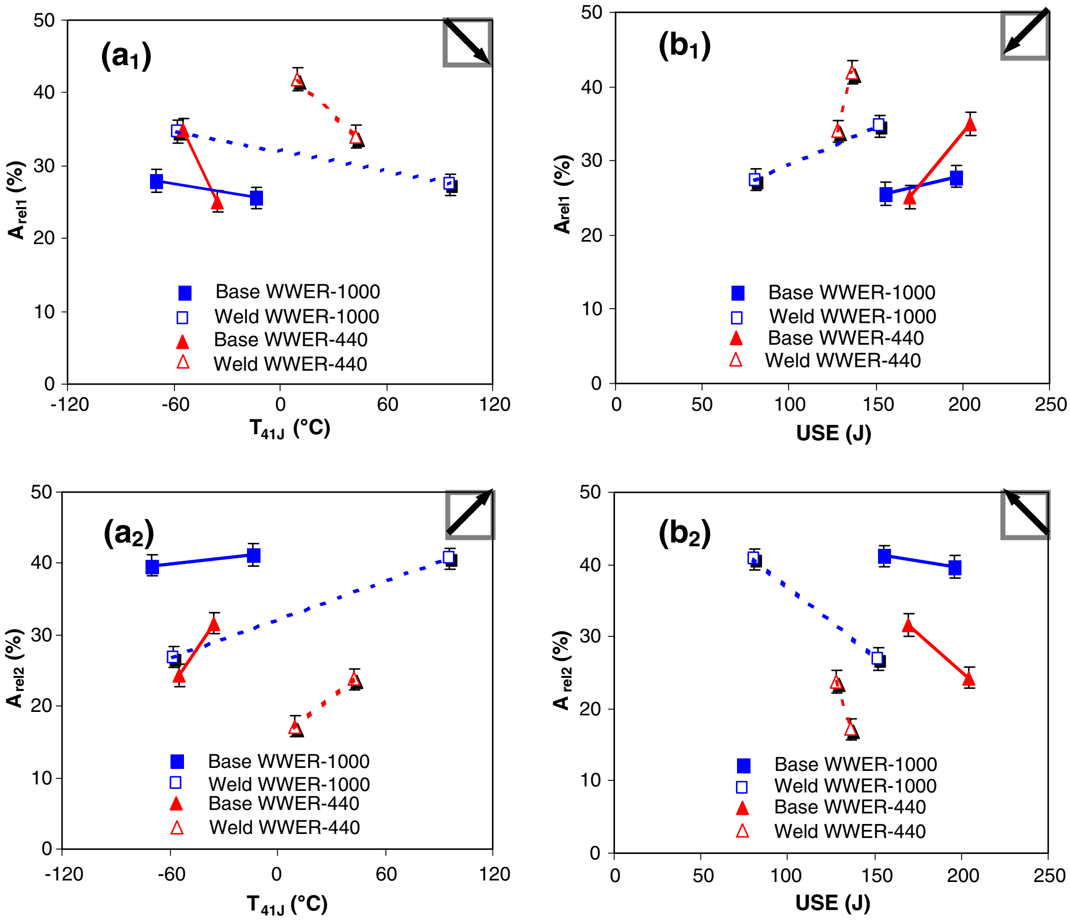

Fig. 5. Change of the relative areas correspond to first (1) and second (2) sextet of Mössbauer spectra versus (a) $T_{41\,\mathrm{J}}$ and (b) USE parameter with irradiation. Arrow indicates the trend-line after irradiation.

Table 3
Summary of the heat treatments and mechanical properties of 15Kh2NMFAA steel

Heat treatment	ΔDBTT (°C)	ΔUSE (J)	ΔHV (a.u.)
Step I			
2 h/600 °C + 2 h/590 °C + 4 h/580 °C + 4 h/570 °C + 6 h/560 °C + 12 h/540 °C + 12 h/530 °C + 12 h/520 °C + 18 h/510 °C + 24 h/500 °C	↑50	↓5	↓5
Step II			
2 h/600 °C + 2 h/590 °C + 4 h/580 °C + 4 h/570 °C + 6 h/560 °C + 12 h/540 °C + 12 h/530 °C + 12 h/520 °C + 18 h/510 °C + 24 h/500 °C + 18 h/510 °C + 24 h/500 °C + 144 h/490 °C + 162 h/480 °C + 96 h/470 °C	↑83	↓50	↑5

considered to be dominated by the direct matrix damage. This conclusion is based on the fact that the amounts of copper and phosphorus are not so high, therefore nickel mainly enhances the matrix damage. Material damage due to direct matrix damage, expressed by the transition temperature shift ($\Delta T_{\mathrm{DMD}} = a \cdot \Phi^n$), is normally proportioned by the square root of the fluence parameter Φ. The MLT shift indicates that it could be related to matrix damage. The situation is rather different if we consider MA-635. Here the damage is probably dominated by the segregation/precipitation of phosphorus, which is present in rather large quantities, while the copper content is negligible. Since the

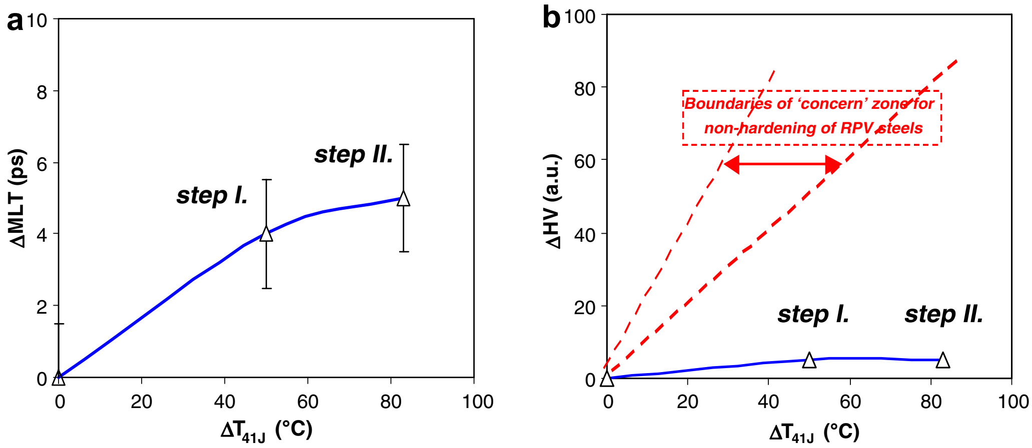

Fig. 6. (a) MLT parameter versus $\Delta T_{41\,J}$, (b) ΔHV versus $\Delta T_{41\,J}$ for RAM samples (15Kh2NMFAA) including the non-hardening zone.

Table 4
Chemical composition of the main alloying elements and impurities (wt%) and mechanical properties of RPV model alloys

Element (wt%)/ Parameter	Model alloy 635	Model alloy 440	Model alloy 175
Ni	0.007	0.71	1.14
P	0.029	0.002	0.01
Cu	0.005	0.4	0.11
Si	0.52	0.17	0.12
Mn	0.5	0.47	0.42
$T_{1.9\,J}$ (°C)	−61.92	−84.05	−54.97
USE (J)	8.28	9.14	8.61

amount of precipitating/segregating elements (P) is finite in the matrix, the process saturates as phosphorus depleted from the matrix. Such saturation behavior of damage in low Ni model alloys has been observed recently, as well as the non-saturation of damage in high Ni model alloys [9,10]. Surprisingly, the MLT increase seems again to be a good qualitative indicator of the process kinetics.

It is noted that MA-175 was much more sensitive to radiation-induced embrittlement than MA-635 (almost double of the $\Delta T_{1.9\,J}$ value was obtained). Unexpectedly, the results for MA-440, where the expected damage is mainly copper precipitation enhanced by nickel, in combination with significant matrix damage, do not saturate [8]. On the contrary, the fitted power function exponent is even rather in excess of the power 1/2 curve. The increase of MLT is anyhow smaller than in the other alloys, in spite of the fact that it proved the most sensitive of the three to radiation embrittlement when irradiated by neutrons. It seems that the MTL increase is sensitive to specific forms of damage; and not primarily to copper-induced damage. For further check these results we compared the available MLT data (Fig. 8(a)) with the fits from the semi-mechanistic model (Eq. (1)) for four different WWER steels

Table 5
Positron lifetime parameters of RPV model alloys for calculated dose level ($Dose_{LT}$)

Model alloy	$Dose_{LT}$ (dpa)	τ_1 (ps)	I_1 (%)	τ_2 (ps)	I_2 (%)	MLT (ps)	VF	HV
MA-635 (Ni) 0.007 wt%	0	104	75.4	216	24.6	131.6	1.31	191
	0.0109	117	79.9	271	20.1	150.0	1.53	158
	0.0260	109	85.5	288	13.5	151.9	1.21	119
MA-440 (Ni) 0.71 wt%	0	114	82.4	225	16.9	142.2	1.15	162
	0.0112	116	84.1	310	15.9	147.0	1.23	138
	0.0258	119	90.1	352	9.4	153.0	0.99	141
MA-175 (Ni) 1.14 wt%	0	114	78.9	170	20.6	136.9	1.29	146
	0.0106	115	82.1	299	17.9	149.0	1.28	140
	0.0286	119	86.8	277	11.9	155.1	1.01	129
Accuracy	–	±2	±0.5	±5	±1	±3	–	±4

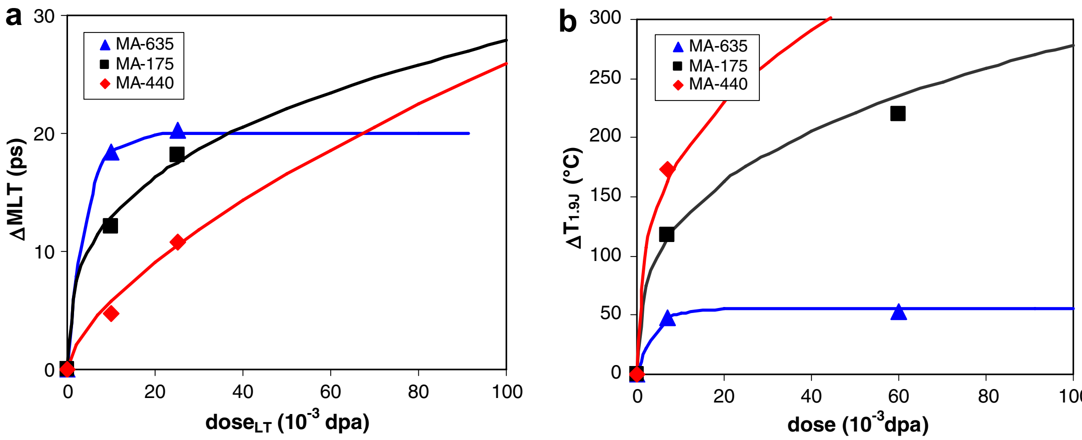

Fig. 7. (a) MLT parameter versus proton dose$_{LT}$ (dpa), (b) shift of $T_{1.9\,J}$ (points – experimental data; line – fits according to the semi-mechanistic models) versus neutron dose for the selected RPV model alloys.

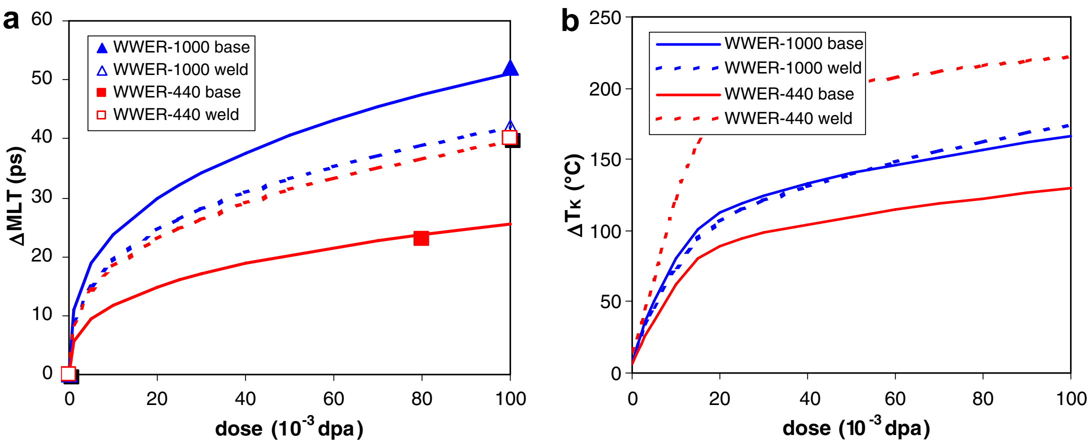

Fig. 8. Fits of the ΔMLT parameters based on the direct matrix damage model correlated with experimental ΔMLT plotted versus (a) proton dose, (b) neutron dose for WWER RPV steels.

(Fig. 8(b)). There is an indication that a similar model, as for model alloys, can also be used in this case. However, it should be emphasized that this is based on a small amount of experimental data. More systematic studies are needed to be done to clarify the extent which increase of MLT can be quantitatively related to the various damage contributions.

4. Conclusion

Different RPV-steel specimens from WWER round robin and surveillance programs and RPV model alloys in various conditions (non-irradiated, irradiated and thermally treated) have been studied using different nuclear spectroscopic methods (PAS and MS). Moreover, the results have been correlated with $T_{41\,J}$ and USE parameters for RPV WWER steels class and with hardness for the model alloys.

The positron lifetime technique significantly demonstrated the capability to be used for evaluation of the radiation damage level caused by irradiation. Comparison of positron mean lifetimes (MLT) showed that irradiated specimens contain a higher concentration of vacancy type defects. The results also confirmed the creation of small radiation-induced defects (point defects such as mono-, di-vacancies or small vacancy clusters and/or interstitials), which were visible in the all specimens examined. This effect was most significant for the WWER-1000 base metal, although there are strong indications that the generation of defects (direct matrix damage) is not the most important degradation process itself. The change of $T_{41\,J}$ and USE parameters is very limited in this case. Therefore, the content of alloying elements and impurities plays a more important role. Anyway, due to irradiation, atoms like Ni, Mn, Cr, Mo became mobile and precipitate in form of carbides and/or Cu- and P-rich precipitates and alloying atoms aggregates. This is registered as a change of relative areas of MS spectra (decrease of A_{re1} and an increase of A_{re2}) that should be explained as a migration of alloying elements and impurities closer to the pure iron matrix. In particular, we assume that the content of nickel affects both the size and distribution of the Cu-rich clusters and precipitates. Nickel also takes part in the composition of these clusters, as well as of the P-rich ones. The effect of manganese and chromium seems to be important too, as they have an influence on the sensitivity of the steel to radiation damage. It is concluded that MS parameters reflect the different chemical composition of iron-based specimens better than PAS, moreover MS is also able to follow irradiation hardening.

In addition to irradiation experiments a special thermal treatment of 15Kh2NMFAA RPV steel was performed to induce the segregation of phosphorus in the microstructure. However, the P-segregation process was not fully detected by positron annihilation probably, due to creation of formations, that could not be detected by positron annihilation. On the other hand we can conclude that observed change of MS parameters was caused mainly by the precipitation process involving atoms as Ni, Mn, Cr, Mo, which become mobile and precipitate in form of carbides and/or Cu- and P-rich phases and alloying atoms aggregates.

Moreover, a consistent correlation of the PAS and MS data was obtained with mechanical testing parameters, such as ductile-to-brittle transition temperature ($T_{41\,J}$) and upper shelf energy (USE) for the steels examined in this study.

The different mechanisms of radiation embrittlement have been studied by nuclear spectroscopic techniques. We can conclude that the radiation damage caused by protons has different effects, as damage due to neutron irradiation. Although, direct matrix damage is common to both types of irradiation, the effects of Cu-precipitation and P-segregation were not confirmed for materials irradiated by protons at these relatively low doses. Nevertheless, more experimental studies are needed for the validation of the observed changes. This research activity is still ongoing and will involve also other techniques as APFIM, TEM and SANS possibly, which seem to be also very essential tools for investigation of the microstructure at the atomic scale.

References

[1] R.G. Odette, G.E. Lucas, ASTM STP 1046 (1990) 343.

[2] W.J. Phythian, C.A. English, J. Nucl. Mater. 205 (1993) 162.

[3] M. Grosse, V. Denner, J. Böhmert, M.-H. Mathon, J. Nucl. Mater. 277 (2000) 280.

[4] J.R. Hawthorne, in: C.L. Briant, S.K. Banerji (Eds.), Treatise on Materials Science and Technology, vol. 25, Academic, New York, 1983, p. 461.

[5] Y.A. Nikolaev, A.V. Nikolaeva, A.M. Kryukov, Y.I. Shtrombakh, P.A. Platonov, in: Proceedings of the TACIS Workshop on the RPV Life Predictions, PCP3-ENUCRA-D4, 2000.

[6] L. Debarberis, U. von Estorff, S. Crutzen, M. Beers, H. Stamm, M.I. de Vries, G.L. Tjoa, Nucl. Eng. Des. 195 (2000) 217.

[7] M. Valo, R. Krause, K. Saarinen, P. Hautojärvi, R. Hawthorne, ASTM STP 1125, Stoller, Philadelphia, 1992.

[8] M.K. Miller, M.G. Burke, J. Nucl. Mater. 195 (1992) 68.

[9] IAEA-TECDOC-1441, Effect of nickel on irradiation embrittlement of light water reactor pressure vessel steels, Vienna, 2005.

[10] V. Slugen, A. Zeman, J. Lipka, L. Debarberis, J. NDT&E Int. 37 (2004) 651.

[11] L. Debarberis, B. Acosta, F. Sevini, A. Kryukov, F. Gillemot, M. Valo, A. Nikolaev, M. Brumovsky, J. Nucl. Mater. 336 (2005) 210.

[12] L. Debarberis, A. Kryukov, F. Gillemot, B. Acosta, F. Sevini, Int. J. Pres. Ves. Pip. 82 (2005) 195.

[13] J. Cizek, I. Prochazka, J. Kocik, E. Keilova, Phys. Status Solidi (a) 178 (2000) 651.

[14] V. Slugen, D. Segers, P.M.A. De Bakker, E. DeGrave, V. Magula, T. Van Hoecke, B. Van Waeyenberge, J. Nucl. Mater. 274 (1999) 273.

[15] P. Hautojäarvi, L. Pöllönen, A. Vehanen, J. Yli-Kauppila, J. Nucl. Mater. 114 (1983) 250.

[16] A. Vehanen, P. Hautojäarvi, J. Johansson, J. Yli-Kauppila, P. Moser, Phys. Rev. B 25 (1982) 762.

[17] G. Brauer, M. Sob, J. Kocik, Report ZfK-647, Rossendorf, 1990.

[18] L. Kupča, P. Beňo, Nucl. Eng. Des. 196 (2000) 81.

[19] L. Debarberis, B. Acosta, A. Zeman, F. Sevini, A. Ballesteros, A. Kryukov, F. Gillemot, M. Brumovsky, Scripta Mater. 53 (2005) 769.

[20] IAEA-TECDOC-1442, Guidelines for Prediction of Irradiation Embrittlement of Operating WWER-4400 Reactor Pressure Vessels, Vienna, 2005.

[21] P.M.A. De Bakker, V. Slugen, E. De Grave, E. Van Walle, A. Fabry, Hyperfine Interact. 110 (1997) 11.

[22] V. Slugen, Nucl. Eng. Des. 235 (2005) 1961.

[23] L. Debarberis, H. Hein, Int. J. Pres. Ves. Pip. 83 (2006) 565.